Potential structural role of non-coding and coding RNAs in the organization of the cytoskeleton at the vegetal cortex of *Xenopus* oocytes

Malgorzata Kloc, Katarzyna Wilk, Diana Vargas, Yuri Shirato, Szczepan Bilinski and Laurence D. Etkin *Development* **132**, 3445-3457.

In Figure 2 of this paper, panel A1 and panel B2 were inadvertently duplicated. Panel A1 has been replaced with the correct panel in the figure reprinted below. There are no changes to the original figure legend, which is accurate. This error in no way effects the conclusions of the study.

The authors apologise to readers for this mistake.

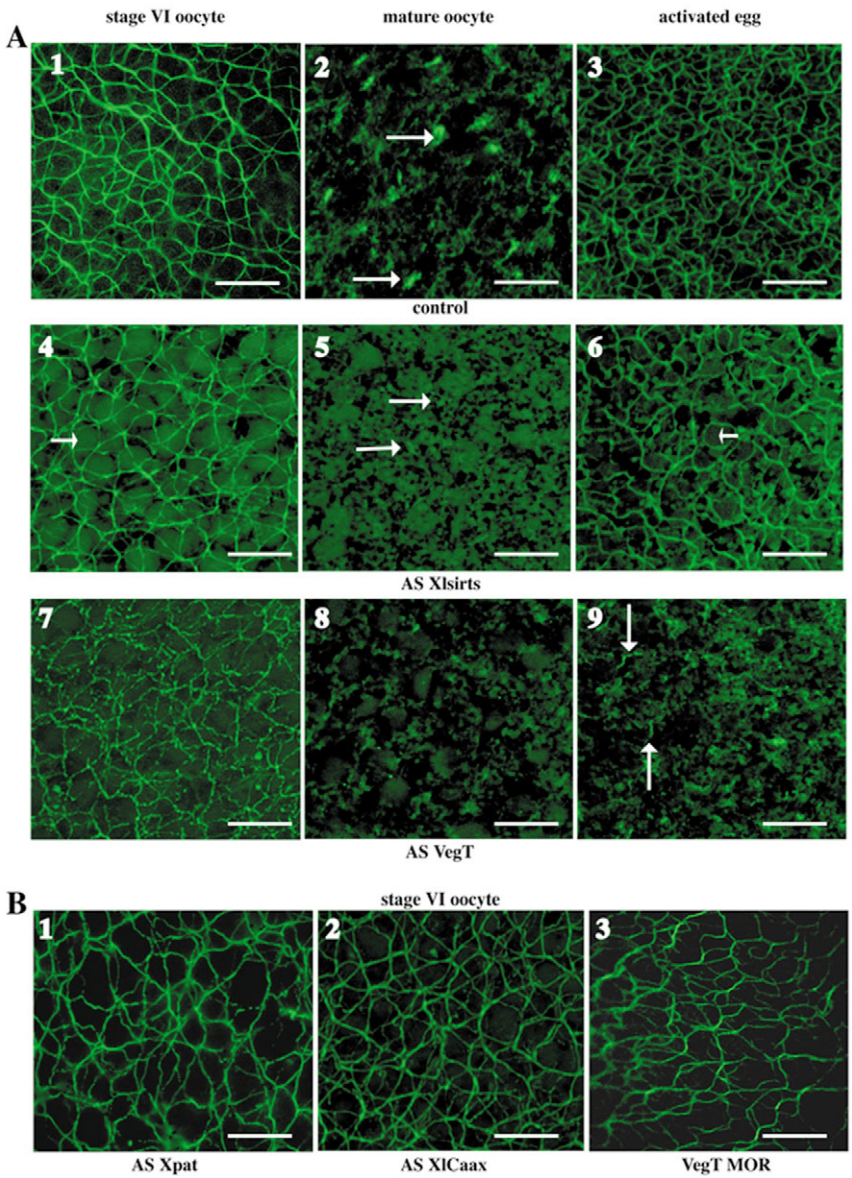

Potential structural role of non-coding and coding RNAs in the organization of the cytoskeleton at the vegetal cortex of *Xenopus* oocytes

Malgorzata Kloc[1], Katarzyna Wilk[2], Diana Vargas[3], Yuri Shirato[1], Szczepan Bilinski[2] and Laurence D. Etkin[1,*]

[1]Department of Molecular Genetics, University of Texas, M. D. Anderson Cancer Center, Houston TX 77030, USA
[2]Institute of Zoology, Jagiellonian University, ul. Ingardena 6, 30-060 Krakow, Poland
[3]Public Health Research Institute, Department of Molecular Genetics, 225 Warren Street, Newark, NJ 07103, USA
*Author for correspondence (e-mail: lde@mdanderson.org)

Accepted 25 May 2005

Development 132, 3445-3457
Published by The Company of Biologists 2005
doi:10.1242/dev.01919

Summary

The localization of RNA within a cell or embryo is crucial for proper cellular function or development. There is evidence that the cytoskeleton and RNA may function in the anchoring of localized RNAs at the vegetal cortex of *Xenopus laevis* oocytes. We found that the organization of the cytokeratin filaments but not the actin cytoskeleton depends on the presence of intact VegT mRNA and a noncoding RNA, Xlsirts. Destruction of either of these transcripts results in disruption of the cytokeratin cytoskeleton in a transcript-specific manner and interferes with proper formation of the germinal granules and subsequent development of the germline. Analysis of the distribution of endogenous VegT and Xlsirts in live oocytes using molecular beacons showed that these RNAs are integrated into the cytokeratin cytoskeleton. These results demonstrate a novel structural role of coding and noncoding RNAs in the organization of the vegetal cortex of *Xenopus* oocytes.

Key words: Localized RNA, Structural role of RNA, Cytokeratin, Germ plasm, *Xenopus*

Introduction

RNAs function in a wide variety of processes in the nucleus and cytoplasm, including regulation of translation, RNA editing and gene regulation. Additionally, a class of localized RNAs found in specific regions of cells or embryos perform many different functions (Bashirullah et al., 1998; Jansen, 2001; Kloc et al., 2002a; Palacios and St. Johnston, 2001).

In *Xenopus laevis*, Vg1 was the first mRNA identified that was localized at the oocyte vegetal cortex (Rebagliati et al., 1985). Now, many different RNAs are known to be localized at the vegetal cortex (Bashirullah et al., 1998; King et al., 1999; Kloc et al., 2002b; Palacios and St. Johnston, 2001). Localized RNAs such as Vg1 (Joseph and Melton, 1998; Kessler and Melton, 1995); the *Xenopus* homolog of Bicaudal-C (Wessely and de Robertis, 2000); and the T-box family member VegT (Xanthos et al., 2001; Zhang and King, 1996) are involved in mesoderm and/or endoderm formation. Recently, Hermes was shown to regulate the cleavages of the vegetal blastomeres (Zearfoss et al., 2004). Xcat2 and Xpat mRNAs are thought to have functions specific to germ cells because of their association with germ plasm, which contains the germ cell determinants within structures called germinal granules (Yisraeli et al., 1990; Kloc and Etkin, 1995; Forristall et al., 1995; Kloc et al., 1998; Kloc et al., 2002a).

Localized RNAs co-fractionate and co-immunoprecipitate with cytoskeletal elements that serve in both RNA transport and anchoring (Alarcon and Elinson, 2001; Boccaccio et al., 1999; Elinson et al., 1993; Forristall et al., 1995; Jankovics et al., 2002; Klymkowsky et al., 1991; Marikawa et al., 1997; Pondel and King, 1988; Shan et al., 2003; Stebbings, 2001; Yisraeli et al., 1990; Zhao et al., 1991). Interestingly, a noncoding RNA, Xlsirts (Kloc and Etkin, 1994) and VegT mRNA (Heasman et al., 2001; Zhang and King, 1996), when destroyed with antisense oligonucleotides (ODNs), caused release of specific RNAs from the vegetal cortex. The present study demonstrates that VegT and Xlsirts RNAs are integrated within the cytokeratin cytoskeleton and that destruction of these RNAs disrupts the cytoskeleton in specific ways resulting in the release of several different RNAs. This suggests the intriguing possibility that both coding and noncoding RNAs may have several roles, including structural organization of the vegetal cortex in *Xenopus* oocytes.

Materials and methods

Animals and oocytes

Xenopus laevis wild-type females were anesthetized and pieces of ovary were surgically removed and placed in oocyte medium (OCM) (Heasman et al., 1991). Stage IV and VI oocytes were defolliculated manually, and injected and incubated in the same medium.

Northern blot

Total RNA was prepared from control and antisense Xpat ODN-injected stage VI oocytes (100 oocytes in each group) using Trizol (Invitrogen) according to manufacturer protocol. Poly(A) RNA was isolated from total RNA using Poly(A)purist kit from Ambion. Northern blot was prepared according to standard methods and

hybridized to digoxigenin-labeled antisense Xpat RNA probe synthesized from Xpat 3′UTR (Xpat3′UTR in Bluescript was a gift from Hugh Woodland, University of Warwick, UK), and antisense Xcat2 probe synthesized from Xcat2-Sport (gift from M. L. King, University of Miami, FL) in ULTRAhyb buffer (Ambion) according to manufacturer protocol.

Antisense oligonucleotides

We injected 10 ng per oocyte of phosphorothioated oligonucleotides (synthesized by Sigma Genosys, Woodlands, TX; modified bases marked by the *) of the following sequences: antisense VegT, 5′ C*A*G*C*AGCATGTACT*T*G*G*C 3′ (Zhang et al., 1998; Heasman et al., 2001); antisense Xlsirts 1, 5′ C*A*G*GTATA-GTAGGG*A*G*A 3′ (Kloc and Etkin, 1994); antisense Xlsirts 2, 5′ T*C*T*CTGGGAAGGGA*G*T*G 3′ (Kloc and Etkin, 1994); antisense XlCaax, 5′ C*T*G*CGCTTAGAGAA*C*C*C 3′ (Kloc and Etkin, 1994); antisense Xpat, 5′ T*T*C*T*GCCTTCAAAGCC-AT*A*G*A 3′; sense VegT, GC*C*A*A*GTACATGCT*G*C*T*G; sense XlCaax, CG*G*T*TCTCTAAGCG*C*A*G; sense Xlsirts 1:TC*T*C*CCTACTATA*C*C*TG; sense Xlsirts 2, CA*C*T*C-CCTTCCCAG*A*G*A (Kloc and Etkin, 1994); VegT morpholino, 5′CCCGACAGCAGTTTCTCATTCCAGC 3′ injected at 30 ng (in 10 nl) per oocyte (see Heasman et al., 2001).

Molecular beacons

Molecular beacons, with 2'-O-methylribonucleotide backbone and Texas Red at the 5′ end and BHQ2 (Black hole quencher 2) at the 3′ end were synthesized as in Bratu et al. (Bratu et al., 2003). The molecular beacon oligonucleotides of the following sequences were injected into the oocytes (10 ng in 10 nl): VegT, 5′ **cacac**CAGCAGCATGTACTTGGC**gtgtg** 3′; a 1:1 mixture of Xlsirts number 1 (5′ **cacac**tCAGGTATAGTAGGGAGA**gtgtg** 3′) and Xlsirts number 2 (5′ **caagt**TCTCTGGGAAGGGAGTG**acttg** 3′); and Xpat, 5′ **caagt** TTCTGCCTTCAAAGCCATAGA**acttg** 3′ (the bold nucleotides are the arm sequences). Injected oocytes were incubated in OCM for 4-6 hours at 18°C. Then, 1 nl of an anti-pancytokeratin-FITC antibody (C11 antibody, Sigma) was injected into oocytes, and the vegetal tip of the oocyte was immediately cut off, mounted in PBS on a microscope slide under a coverslip and observed under a Nikon fluorescence microscope within 15-30 minutes of C11-FITC injection.

Host transfer and rescue

Host transfer and rescue was carried out according to Heasman et al. (Heaseman et al., 1991) and Zearfoss et al. (Zearfoss et al., 2004).

Cytoskeleton staining

Actin was stained using rhodamine-phalloidin (Molecular Probes) (Kloc et al., 2004). Cytokeratin immunostaining was carried out according to the method of Alarcon and Elinson (Alarcon and Elinson, 2001).

In situ hybridization

Light and electron microscopy of whole-mount in situ hybridization of oocytes and embryos were performed as described by Kloc and Etkin (Kloc and Etkin, 1994) and Kloc et al. (Kloc et al., 2002a).

Results

To determine how Xlsirts and VegT may function in anchoring other RNAs, we depleted Xlsirts RNA and VegT mRNA using antisense oligodeoxynucleotides (ODNs). Destruction of either VegT or Xlsirts resulted in release of Vg1 mRNA from the vegetal cortex of stage VI oocytes (Fig. 1A,B) consistent with previous studies showing Vg1 mRNA being released and not degraded after destruction of specific RNAs (Kloc et al., 1994; Heasman et al., 2001). Injection of antisense ODNs against another localized mRNA, Xpat did not cause the release of Vg1 RNA (Fig. 1A). Fig. 1C shows that antisense Xpat ODN destroys Xpat mRNA.

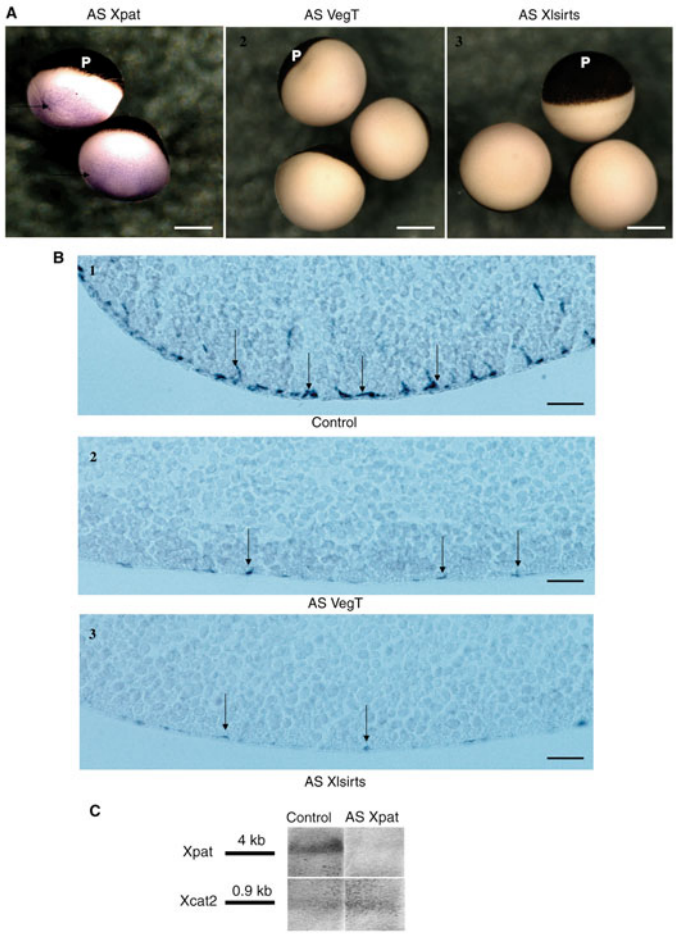

Fig. 1. Destruction of Xlsirts or VegT, but not Xpat RNA, releases Vg1 mRNA from the cortex. (A) Stage VI oocytes analyzed by whole-mount in situ hybridization with digoxigenin-labeled Vg1 probe. (1) Control oocytes injected with antisense Xpat ODN. P, pigmented animal pole; arrows indicate non-pigmented vegetal pole with localized Vg1 mRNA. (2) Oocytes injected with antisense VegT ODN or (3) antisense Xlsirts ODNs. (B) Sections showing the fragments of vegetal cortex of control non-injected (1), antisense VegT- (2) and antisense Xlsirts- (3) injected stage VI oocytes. Arrows indicate Vg1 mRNA at the vegetal cortex in control oocyte and remnants of Vg1 mRNA at the vegetal cortex in antisense Xlsirts- and antisense VegT-injected oocytes. Scale bar: 380 μm in A; 30 μm in B. (C) Northern blot of poly(A)RNA isolated from 100 control and antisense Xpat ODN-injected oocytes, hybridized to antisense Xpat and antisense Xcat2 digoxigenin-labeled probes.

Destruction of Xlsirts or VegT RNA disrupts the cytokeratin network

We hypothesized that the release of Vg1 RNA from the vegetal cortex in VegT or Xlsirts depleted oocytes was caused by disruption of the oocyte cortical cytoskeleton. Therefore, we investigated the effect of destruction of Xlsirts and VegT RNAs on the organization of the cytokeratin and the actin cytoskeleton within the vegetal cortex of full-grown stage VI oocytes, oocytes that were matured in vitro by addition of

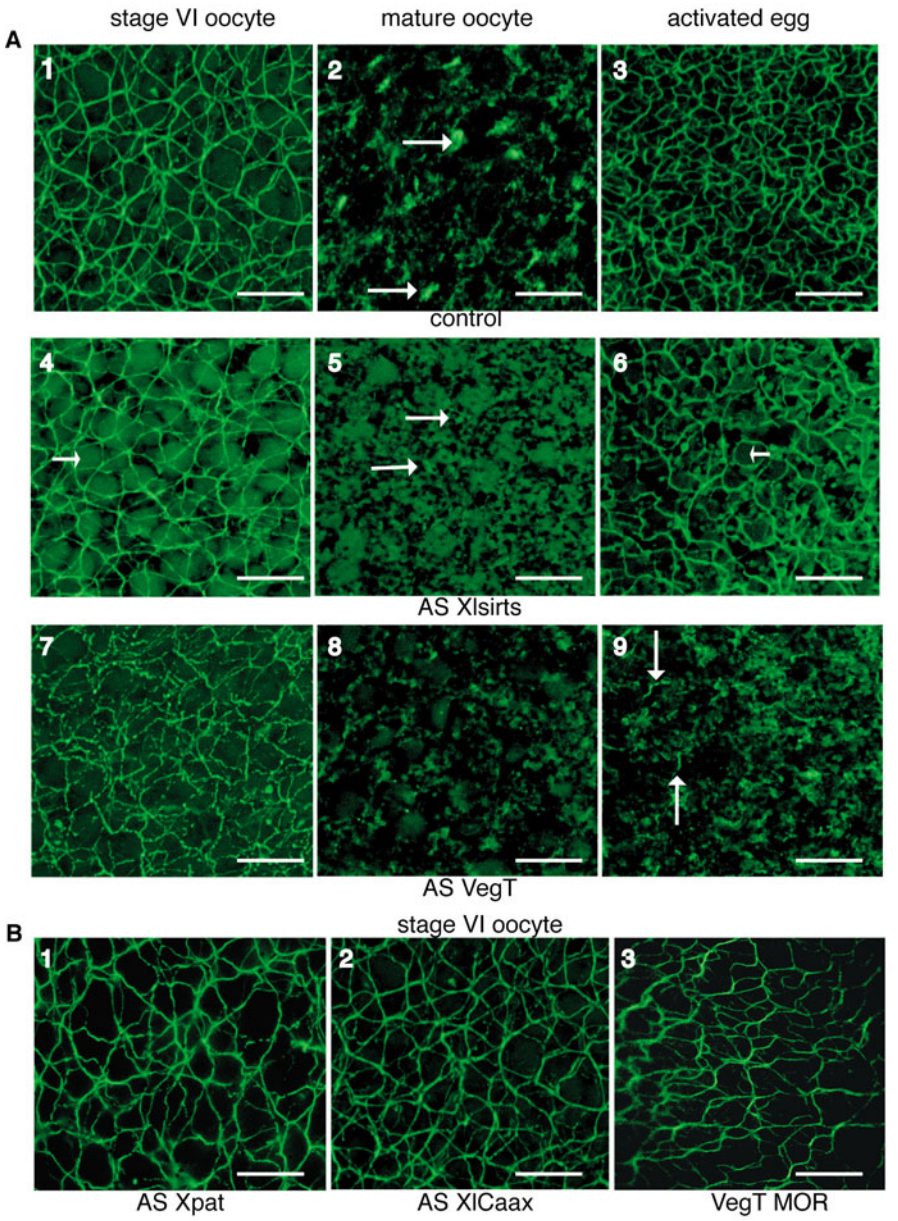

Fig. 2. Cytokeratin in vegetal cortex of stage VI oocytes. (A) Confocal images of the vegetal cortex of stage VI oocytes, oocytes matured *in vitro* and eggs activated by pricking stained with anti-pancytokeratin C11 antibody conjugated with FITC. Left panel, stage VI oocytes. Central panel, oocytes matured *in vitro* with progesterone. Right panel, activated eggs. Control mock-injected stage VI (1) and matured (2) oocytes (arrows indicate cytokeratin foci). (3) Control oocyte after activation. (4) Stage VI oocyte injected with antisense Xlsirts ODNs (short arrow indicates yolk platelet). (5) Matured antisense Xlsirts-injected oocyte (arrows indicate cytokeratin foci). (6) Activated egg from antisense Xlsirt-injected oocyte (short arrow indicates yolk platelet). (7) Stage VI oocyte injected with antisense VegT ODN. (8) Antisense VegT ODN-injected oocyte that has matured. (9) Activated antisense VegT-injected egg showing only separated short filaments of cytokeratin (arrows). (B) Stage VI oocyte injected with antisense Xpat (1), antisense XlCaax (2) ODNs or VegT morpholino (3). Scale bars: 12 μm.

progesterone, and mature oocytes that were activated by pricking with a glass needle.

In control stage VI oocytes the cytokeratin cytoskeleton is visible as an intricate network within the vegetal cortex (Fig. 2A, part 1). During maturation of control stage VI oocytes this network is disrupted, resulting in a punctate appearance consisting of foci of cytokeratin (Fig. 2A, part 2). Following activation by pricking with a glass needle the cytokeratin reforms into a more complex network-like arrangement (Fig. 2A, part 3) (Clarke and Allan, 2003; Klymkowsky et al., 1991; Klymkowsky and Maynell, 1989).

The depletion of Xlsirts or VegT RNA with specific ODNs in stage VI oocytes caused the disruption of the cytokeratin network at the oocyte vegetal cortex (Fig. 2A). Interestingly, the effects of VegT depletion and Xlsirts depletion were different. Destruction of Xlsirts RNA caused a very pronounced 'thinning' or 'flattening' of the cytokeratin network and its collapse inward towards the yolk mass (Fig. 2A, part 4). The cytokeratin network looked well organized but much thinner and less 'three dimensional' than the network in control oocytes, and, in contrast to the control oocytes, the yolk platelets were clearly visible below the cytokeratin network (Fig. 2A, part 4). Destruction of VegT mRNA resulted in fragmentation and disruption of the cytokeratin network (Fig. 2A, part 7).

To analyze the effect of destruction of Xlsirts and VegT RNAs during the processes of maturation and activation, the antisense ODNs were injected into stage VI oocytes, and injected oocytes were incubated for 24 hours, matured by addition of progesterone and activated by pricking. After maturation, cytokeratin foci were sporadically visible in antisense Xlsirts eggs and very rarely visible or not visible at all in antisense VegT egg (Fig. 2A, parts 5 and 8). Upon activation, the cytokeratin network was partially reconstituted in antisense Xlsirts-injected eggs but was less regular than the network in control eggs (Fig. 2A, part 6). However, in antisense VegT activated eggs the cytokeratin network was not reconstituted, and only a few short cytokeratin filaments were visible (Fig. 2A, part 9).

Destruction of vegetally localized Xpat mRNA, a non-localized RNA XlCaax, and sense oligonucleotides against all of the RNAs had no effect on the appearance of the cytokeratin network (Fig. 2B, parts 1 and 2). Injection of VegT morpholino that inhibits translation of VegT protein (Heasman et al., 2001) had no effect on the cytokeratin network in stage VI oocytes (Fig. 2B3) or during maturation and activation (data not shown). These findings support the conclusion that disruption

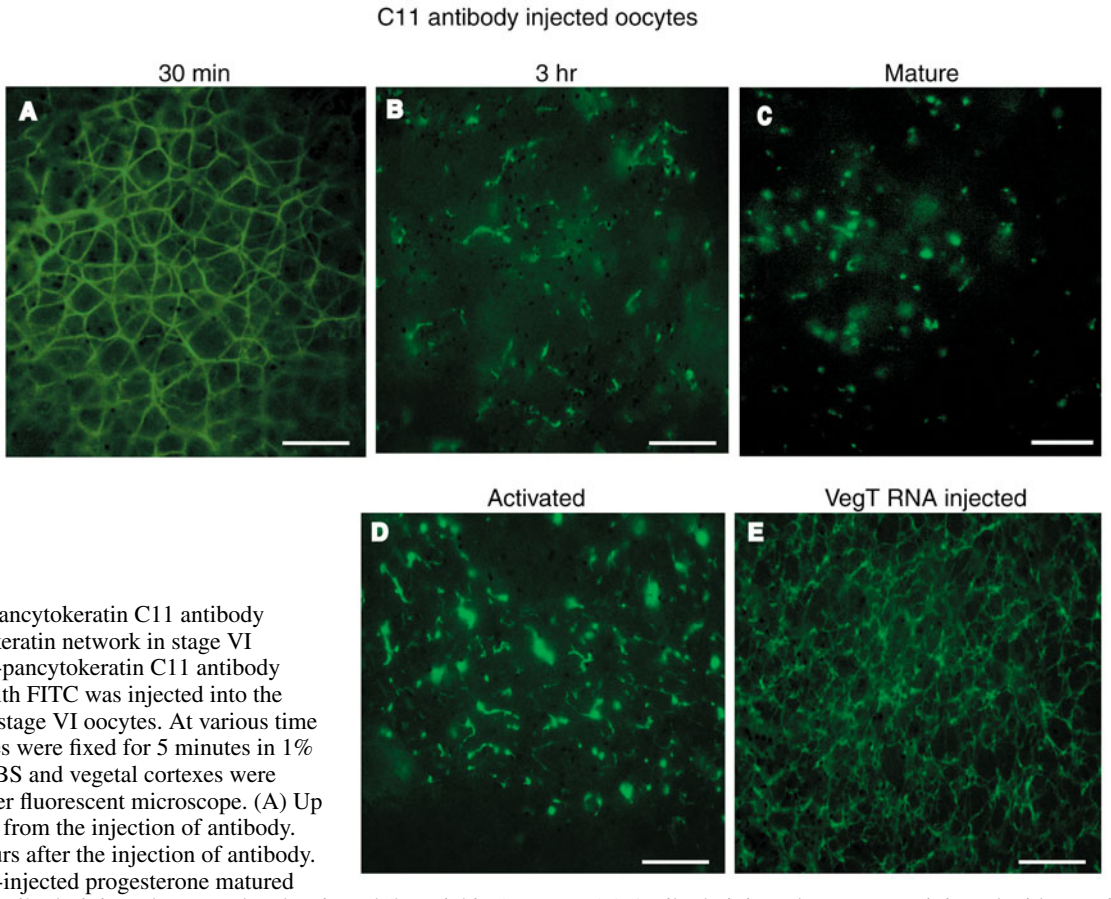

Fig. 3. Anti-pancytokeratin C11 antibody disrupts cytokeratin network in stage VI oocytes. Anti-pancytokeratin C11 antibody conjugated with FITC was injected into the cytoplasm of stage VI oocytes. At various time points, oocytes were fixed for 5 minutes in 1% formalin in PBS and vegetal cortexes were observed under fluorescent microscope. (A) Up to 30 minutes from the injection of antibody. (B) Three hours after the injection of antibody. (C) Antibody-injected progesterone matured oocyte. (D) Antibody-injected, matured and activated (by pricking) oocyte. (E) Antibody injected oocyte post-injected with rescuing VegT RNA shows partial reconstitution of the cytokeratin network. Scale bars: 12 μm.

of the cytokeratin network in oocytes injected with antisense VegT oligonucleotides is due to elimination of RNA and not protein. In addition, no noticeable effect on the cortical actin microfilament cytoskeleton was observed in oocytes, maturing oocytes or activated eggs when XlCaax, Xlsirts or VegT was depleted (data not shown).

We also compared the effects of injection of the anti-pancytokeratin C11 antibody that blocks cytokeratin function (Alarcon and Elinson, 2001) on the cytokeratin network in stage VI oocytes, with those observed after the injection of antisense Xlsirts and antisense VegT ODNs. Thirty minutes after the injection of C11-FITC antibody, the cytokeratin network remained comparable with the control (Fig. 3A). However, ~40 minutes. after the injection of antibody, the network started to disintegrate and, after 3 hours, its remnants were visible as the brightly fluorescing foci (Fig. 3B). When antibody-injected oocytes were matured overnight, the cytokeratin foci, similar to the punctate foci observed in control matured oocytes were visible (Fig. 3C). Following activation, the cytokeratin partially reformed into short filaments, but in contrast to control activated eggs, it did not reform the network-like arrangement (Fig. 3D). These results showed that the disruption of cytokeratin network by anti-pancytokeratin antibody, had similar, although not identical, effects to the disruption of cytokeratin caused by the injection of antisense VegT.

Endogenous Xlsirts RNA and VegT mRNA are components of the cytokeratin network

We also determined the relationship between Xlsirts RNA, VegT RNA and the cytokeratin network. Upon injection of Texas Red-labeled RNAs into vegetal region of stage VI oocytes, the Xlsirts, VegT and Xpat RNAs formed particles measuring 0.5-1.0 μm; however, only Xlsirts and VegT particles had an affinity to the cytokeratin and aggregated on its filaments (Fig. 4A). The difference between the number of Xlsirt, VegT and control Xpat particles aggregated on cytokeratin filaments was statistically significant (Fig. 4B).

Although these results were informative, they did not provide any indication of the distribution of endogenous RNAs in relation to cytokeratin filaments. To investigate the spatial distribution of endogenous Xlsirts and VegT RNAs on the cytokeratin network, we used the technique of in vivo in situ hybridization with molecular beacons (Fig. 5). Molecular beacons are short synthetic hairpin 2′-O-methylribonucleotides complementary to their cellular RNA targets that possess a fluorophore on one end of the molecule and a quencher on the other end. The hairpin configuration holds the fluorophore and quencher in close proximity, thus blocking the fluorescence signal. Upon injection into an oocyte and binding to the cognate RNA, the hairpin configuration becomes disrupted such that the fluorophore is removed from the vicinity of the quencher and the fluorescence of the probe

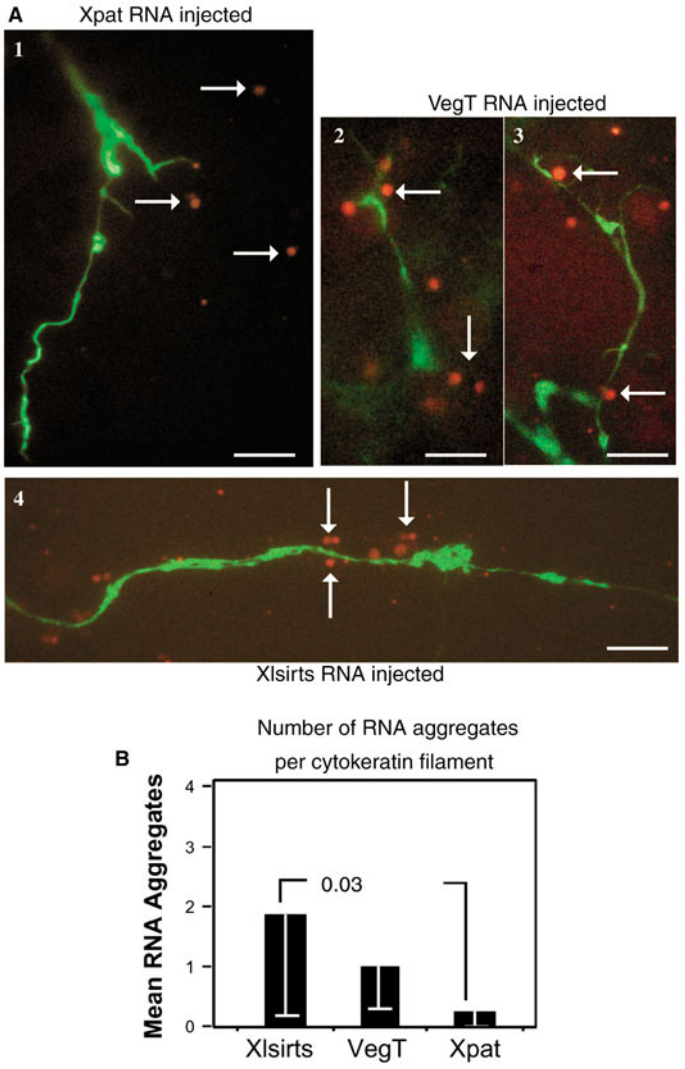

Fig. 4. Association of injected Xlsirts and VegT RNAs with the cytokeratin filaments in stage VI oocytes. (A) Texas Red-labeled synthetic RNA (red) was injected into stage VI oocytes, cytokeratin was labeled with FITC-conjugated antibody (green), and vegetal cortices were observed under a fluorescence microscope. In Xpat RNA-injected oocytes, particles of Xpat RNA were visible outside of cytokeratin filaments (1, arrows). In VegT RNA-injected (2,3) and Xlsirts RNA-injected (4) oocytes, RNA particles were concentrated around and on the cytokeratin filaments (arrows). Scale bar: 500 nm. (B) Student's *t*-test statistical analysis of the number of RNA aggregates associated with cytokeratin filaments showing the statistically significant difference (P=0.03) between the number of aggregates in VegT and Xlsirts versus Xpat RNA-injected samples. Each bar represents the average (with the standard deviation) number of RNA aggregates counted in eight independent samples along the 2 μm length of cytokeratin filament in each experimental group.

is restored (Bratu et al., 2003; Marras et al., 2004; Tyagi and Kramer, 1996).

We injected Texas Red-conjugated molecular beacons against Xlsirts, VegT and Xpat RNAs into stage VI oocytes. After a 6-hour incubation we injected an anti-pancytokeratin C11-FITC antibody, and within 30 minutes, we examined the distribution of molecular beacons bound to their target RNAs in relation to the cytokeratin network. We found that the pattern of distribution differed for each of the three RNAs. Xlsirts RNA formed two different types of aggregates: smaller ones intimately associated with cytokeratin (Fig. 5A, parts 1 and 2) and much larger ones that we believe represent the germ plasm islands (data not shown). VegT mRNA formed an intricate network of bright foci or aggregates associated with cytokeratin filaments (Fig. 5A, parts 3 and 4). Very often the regular spacing of the VegT RNA on cytokeratin filaments was clearly visible (Fig. 5A, part 4). By contrast, Xpat mRNA, was absent from the cytokeratin network and was present only in large aggregates that probably represented the germ plasm islands (Fig. 5A, part 5; not shown). Statistical analysis of frequency of association of RNA particles with cytokeratin filaments confirms these results (Fig. 5B). In addition, VegT and Xlsirts RNAs were detected in particles that measured ~0.5-1.0 μm in diameter. This is very similar to the size of the particles formed from injected Xlsirts and Vg1 RNAs while they were translocating to the vegetal cortex (Kloc et al., 1996).

The results of our analysis indicate that endogenous VegT mRNA and Xlsirts RNA are components of the cytokeratin network in the vegetal cortex of stage VI *Xenopus* oocytes, and that the two RNAs have unique patterns of association with cytokeratin filaments. Although our results do not demonstrate if the interaction with the cytoskeleton is direct or indirect, they do demonstrate the presence of these RNAs within the cytokeratin network.

Exogenous VegT RNA is able to reconstitute and rescue the disrupted cytokeratin network

We next wanted to see if the cytokeratin network disintegrated by the depletion of VegT mRNA could be reconstituted and rescued upon the injection of VegT RNA. Stage IV and VI oocytes were injected with antisense VegT ODN, followed by injection with VegT mRNA known to rescue antisense VegT depletion (Zhang and King, 1996; Heasman et al., 2001; Horb and Thomsen, 1997). The rationale behind injection into stage IV oocytes was that stage IV oocytes (in contrast to stage VI oocytes) are able to localize injected RNA to the vegetal cortex (Yisraeli and Melton, 1988). The cytokeratin network in vegetal cortex of control stage IV oocytes differs significantly in appearance from the network of stage VI oocytes (Clarke and Allan, 2003); it is irregular and much less intricate (Fig. 6A,B), thus the disruption of the network upon antisense VegT ODN injection into stage IV oocytes causes seemingly much less dramatic effect than in stage VI oocytes (Fig. 6C,D).

The exogenous VegT mRNA, but not Xpat or Vg1 mRNA, was able to reconstitute and rescue the cytokeratin network in stage IV and stage VI oocytes (Fig. 6E,F; data not shown). Interestingly, the reconstituted network in stage IV oocytes was strikingly more complex and multidimensional than in controls, and similar to the network in stage VI oocytes (Fig. 6E,F). The rescuing effect of VegT mRNA occurred not only in stage IV but also in stage VI oocytes, when injected RNA is unable to localize. Thus, the ability of RNA to localize was irrelevant for rescue. We also found that the exogenous VegT RNA was able to reconstitute, to considerable extent, the cytokeratin network in the oocytes injected with anti-pancytokeratin C11 antibody (see Fig. 3E). In addition, we found that the injection of VegT RNA did not change the cytokeratin network appearance when injected to control

oocytes (Fig. 6G,H). This result, and the fact that VegT RNA also reconstitutes the network in antibody-injected oocytes, suggests that the rescuing effect of VegT RNA operates at the level of cytokeratin network-subunit assembly.

Disruption of the cytokeratin network interferes with the formation of the germinal granules and subsequent development of the primordial germ cells

We next investigated the biological consequences of disruption of the cytokeratin cytoskeleton. Residing at the vegetal cortex are the germinal granules, which are components of the germ plasm that specifies the germ cell lineage. Germinal granules are electron-dense structures that contain several different RNAs, including Xcat2 and Xpat. The Xlsirts RNA is located within the germ plasm in the germ plasm matrix between the germinal granules (Hudson and Woodland, 1998; Kloc et al., 2001; Kloc et al., 2002b).

As the depletion of Xlsirts and VegT RNAs affects the organization of the germ plasm-containing region of the vegetal cortex, we analyzed the effect of depletion of these RNAs on the morphogenesis of the germinal granules in matured oocytes, activated eggs and embryos of different stages acquired by host transfer (Heasman et al., 1991). Stage VI oocytes injected with either Xlsirts, VegT, XlCaax antisense ODNs, VegT morpholino or anti-pancytokeratin C11 antibody, were incubated for 24 hours, matured and placed within the host female. In matured and activated eggs originating from control, antisense XlCaax, antisense Xlsirts and VegT morpholino-injected oocytes, the germ plasm and germinal granules appeared normal at the electron microscopic level (Fig. 7A-D). However, in antisense VegT injected oocytes, the germinal granules were strikingly abnormal, forming long intricate chains of electron dense material (Fig. 7E) that looked similar to the germinal granule aggregates normally present much later in cleaving embryos (Kloc et al., 2002b). This finding suggested that the depletion of VegT mRNA (but not VegT protein) from the oocyte cortex causes untimely and premature aggregation of the germinal granules.

Next, we analyzed the effect of Xlsirts and VegT depletion, and the effect of anti-cytokeratin antibody on germinal granule structure and on the association of Xcat2 mRNA with the granules in early embryos. Although the appearance of the germ plasm in whole mounts was similar in control and antisense ODN-injected embryos, the intensity of Xcat2 labeling was clearly lower in antisense Xlsirts embryos (Fig. 8A, parts 1 and 2). Higher magnification revealed that in antisense Xlsirts-injected embryos, the Xcat2 mRNA was

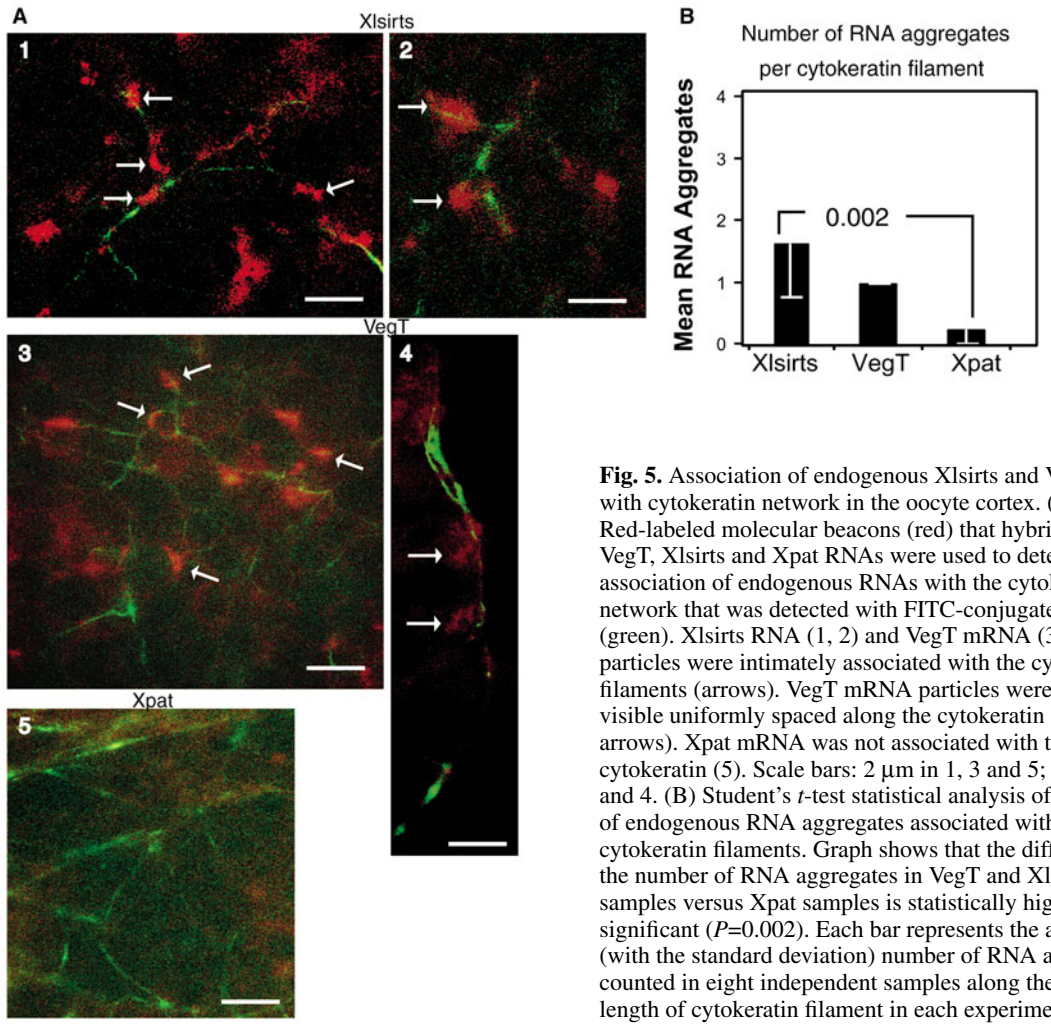

Fig. 5. Association of endogenous Xlsirts and VegT RNAs with cytokeratin network in the oocyte cortex. (A) Texas Red-labeled molecular beacons (red) that hybridize to VegT, Xlsirts and Xpat RNAs were used to detect the association of endogenous RNAs with the cytokeratin network that was detected with FITC-conjugated antibody (green). Xlsirts RNA (1, 2) and VegT mRNA (3, 4) particles were intimately associated with the cytokeratin filaments (arrows). VegT mRNA particles were often visible uniformly spaced along the cytokeratin filament (4, arrows). Xpat mRNA was not associated with the cytokeratin (5). Scale bars: 2 μm in 1, 3 and 5; 1.2 μm in 2 and 4. (B) Student's *t*-test statistical analysis of the number of endogenous RNA aggregates associated with cytokeratin filaments. Graph shows that the difference in the number of RNA aggregates in VegT and Xlsirts samples versus Xpat samples is statistically highly significant (P=0.002). Each bar represents the average (with the standard deviation) number of RNA aggregates counted in eight independent samples along the 2 μm length of cytokeratin filament in each experimental group.

present in the germ plasm region but was located outside of the germinal granules, which were mostly unlabeled thus barely visible. Labeled granules were observed only sporadically, and the labeling intensity was lower than in control embryos (Fig. 8B, parts 1 and 2; see Fig. 10A, parts 3 and 3′; Fig. 10B). By contrast, the germ plasm of antisense VegT or anti-pancytokeratin antibody injected embryos, instead of containing a high number of small aggregates, contained a lower number of large stringy aggregates of labeled germinal granule-like structures (Fig. 8A, parts 3 and 4; Fig. 8B, parts 3 and 4). Interestingly, the cytokeratin network was present not only in control embryos but also in the embryos originating from antisense VegT, antisense Xlsirts and anti-pancytokeratin antibody injected eggs (Fig. 9). This indicates that disruption of the cytokeratin network in oocytes and eggs does not prevent the reconstitution of a seemingly normal network during cleavage, and shows that the untimely aggregation of germinal granules in antisense VegT-injected embryos is a consequence of the disruption of the cytokeratin network in the oocytes and not in the embryos.

The ultrastructure of germinal granules in antisense and anti-cytokeratin antibody injected embryos was analyzed at the electron microscopic level (Fig. 10A). In embryos injected with antisense XlCaax or antisense Xpat ODNs, the Xcat2 mRNA was located throughout the germinal granule and no abnormalities were detected (Fig. 10A, parts 1, 2, 1′, 2′; not shown). In antisense Xlsirts embryos, the germinal granules were largely devoid of Xcat2 mRNA (Fig. 10A, parts 3 and 3′; Fig. 10B). However, in antisense VegT ODN-injected embryos, Xcat2 mRNA remained partially on the granules, which now resembled abnormally large aggregates (Fig. 10A, part 4). These were probably formed by the further aggregation of untimely coalesced stringy aggregates present in VegT-depleted oocytes (see Fig. 7E). The germinal granules in anti-pancytokeratin antibody-injected embryos formed large aggregates that were similar, but not identical, to the germinal granules aggregates in antisense VegT embryos (Fig. 10A, part 5). However, in contrast to antisense VegT embryos, the amount of Xcat2 mRNA in anti-pancytokeratin antibody embryos was similar to control embryos (Fig. 10B). Statistical analysis of Xcat2 mRNA distribution within the germinal granules of control and experimental embryos showed that the number of Xcat2 mRNA grains (silver grains) per 0.25 μm^2 area of germinal granule was similar in control, anti-cytokeratin C11 antibody and antisense Xpat ODN-injected embryos, and significantly lower in antisense VegT ODN- and antisense Xlsirts ODNs-injected embryos (Fig. 10B). Thus, disruption of the cytokeratin network within the vegetal cortex of stage VI oocytes by either depletion of Xlsirts and VegT RNAs or by the injection of anti-pancytokeratin antibody has a major effect on the formation, structure and molecular composition of the germinal granules. This indicates an important link between the structural integrity of the vegetal cortex and subsequent events that occur during development, supporting our conclusion that Xlsirts and VegT RNAs do function in the maintenance of the cytokeratin network in the oocyte cortex.

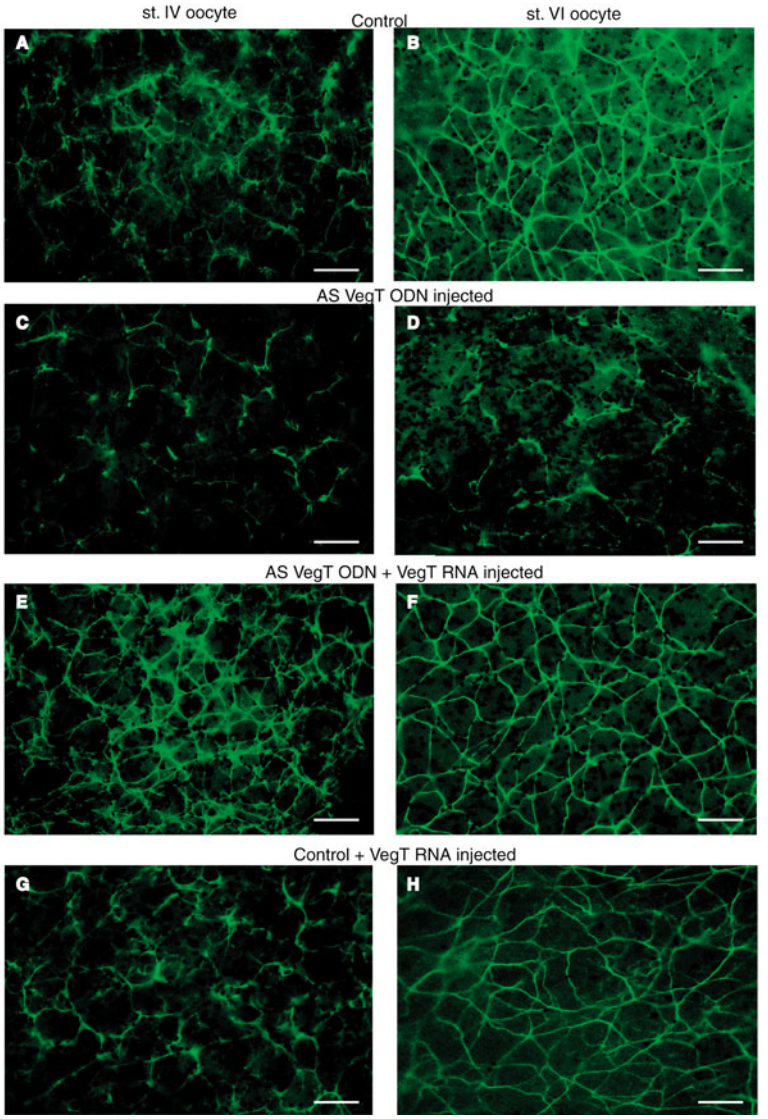

Fig. 6. Injected VegT RNA rescues and reconstitutes the cytokeratin network disintegrated by antisense VegT oligonucleotides. Cytokeratin network in control stage IV oocytes (A) and stage VI oocytes (B). (C) antisense VegT ODN-injected stage IV and (D) stage VI oocytes. After the injection of synthetic VegT RNA, the cytokeratin network reconstitutes as a more complex network in stage IV oocytes (E) and as a normal (comparable with control) network in stage VI (F) oocytes. The injection of synthetic VegT RNA into control stage IV (G) and stage VI (H) oocytes does not affect the appearance of the cytokeratin network. Scale bars: 12 μm.

To further assess developmental defects, we analyzed primordial germ cells (PGCs) in embryos produced by the host transfer method following depletion of Xlsirts or VegT RNA in stage VI oocytes. Xpat mRNA was used as a marker to identify PGCs (Hudson and Woodland, 1998). In agreement with Heasman et al. (Heasman et al., 2001) and Zhang and King (Zhang and King, 1996), antisense VegT injected embryos are unable to undergo gastrulation or neurulation properly; therefore, we analyzed PGCs in blastula

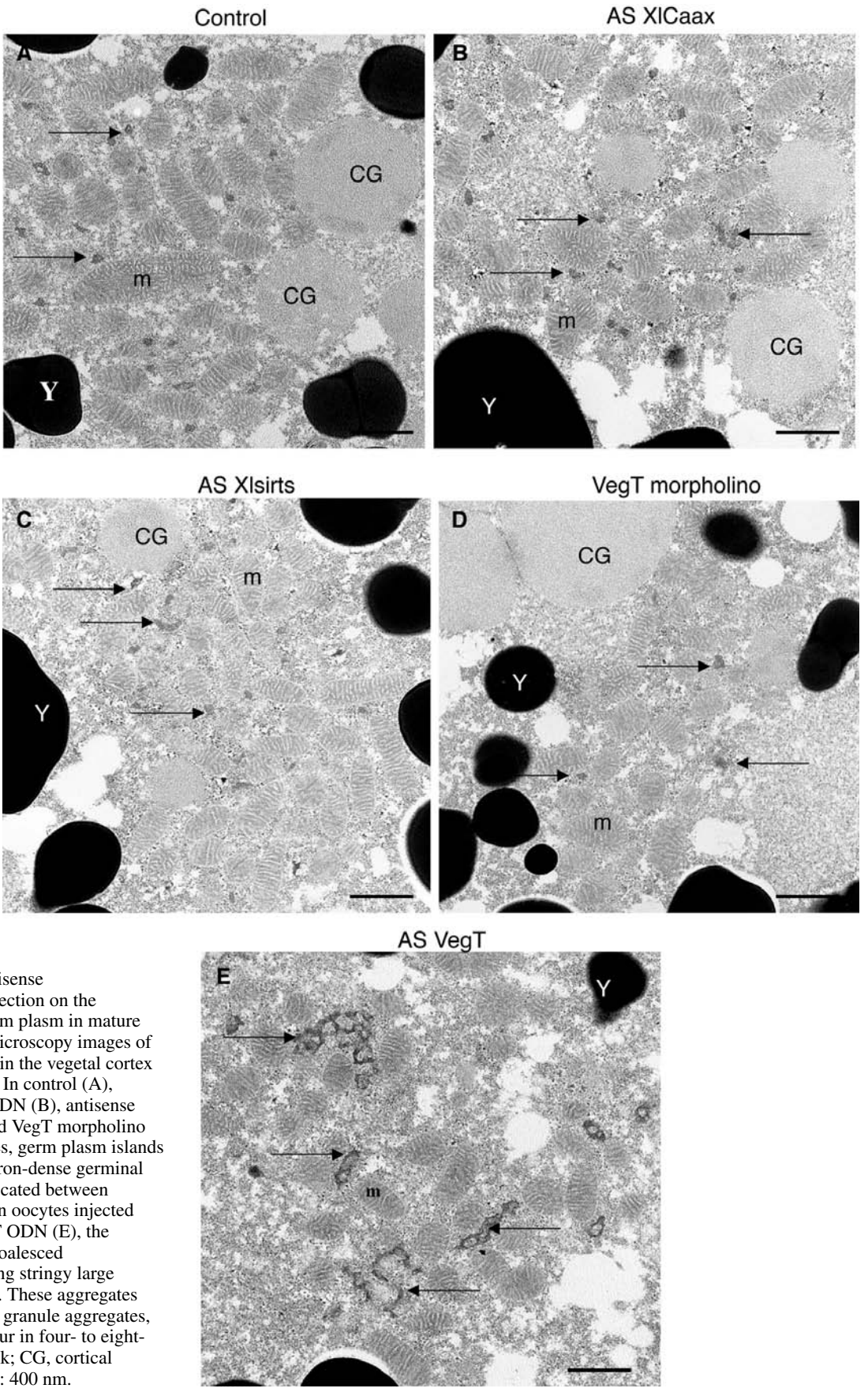

Fig. 7. Effect of antisense oligonucleotides injection on the ultrastructure of germ plasm in mature oocytes. Electron microscopy images of germ plasm islands in the vegetal cortex of matured oocytes. In control (A), antisense XlCaax ODN (B), antisense Xlsirts ODN (C) and VegT morpholino (D) -injected oocytes, germ plasm islands contained tiny electron-dense germinal granules (arrows) located between mitochondria (m). In oocytes injected with antisense VegT ODN (E), the germinal granules coalesced precociously, forming stringy large aggregates (arrows). These aggregates resembled germinal granule aggregates, which normally occur in four- to eight-cell embryos. Y, yolk; CG, cortical granules. Scale bars: 400 nm.

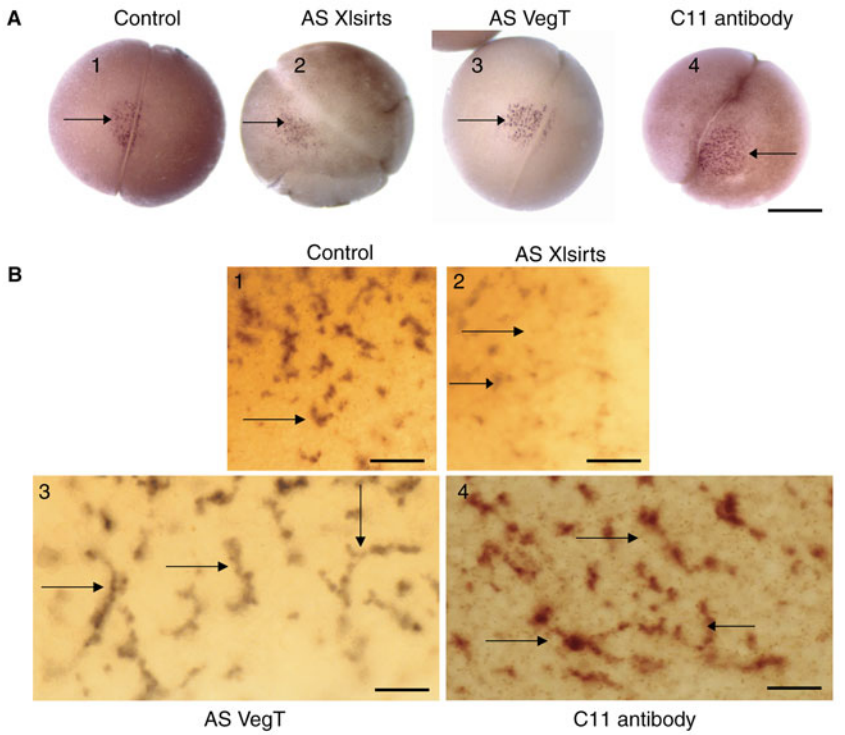

Fig. 8. Effect of antisense oligonucleotides and anti-pancytokeratin C11 antibody injection on germ plasm and germinal granules in two-cell embryos. (A) Whole-mount in situ hybridization with digoxigenin-labeled antisense Xcat2 RNA probe showing the Xcat2 RNA present in the germinal granules within the germ plasm (arrows). Germ plasm of control (1), antisense Xlsirts ODNs (2), antisense VegT ODN (3) and anti-pancytokeratin C11 antibody (4) -injected embryos. (B) Higher magnification of germ plasm regions showing Xcat2 labeled germinal granules in control embryos (1, arrow); unlabelled or slightly labeled granules in antisense Xlsirts embryos (2, arrows); and labeled large stringy aggregates of germinal granules in antisense VegT (3, arrows) and anti-pancytokeratin C11 antibody (4, arrows) embryos. Scale bars: 340 μm in A; 25 μm in B.

embryos. This, at least partially, eliminated the possibility that changes in PGCs were a consequence of an abnormal development. It is known that in mid to late blastula embryos (stage 7-9), the dividing PGCs occupy the vegetal tip of blastula. At this stage the germ plasm is visible as small aggregates, on the vegetal tip of blastula (Fig. 11A) (Hudson and Woodland, 1998). In VegT-depleted embryos, the germ plasm was visible as a single large aggregate (reminiscent of large aggregates present in early embryos) and as smaller dispersed aggregates (Fig. 11B,C). In Xlsirts-depleted embryos, the germ plasm was either barely visible or visible as tiny germ plasm islands scattered throughout the vegetal blastomeres instead of being found in compact group (Fig. 11D,E). Therefore, disruption of the cytokeratin network within stage VI oocytes not only affected the formation of the germinal granules but also had a direct consequence on the appearance and behavior of the germ plasm and possibly on the formation of the primordial germ cells in later-stage embryos, as judged by the distribution of Xpat mRNA within the germ plasm of blastula PGCs.

Discussion

Our data support a model in which the non-coding Xlsirts RNA and the coding VegT mRNA play a structural role in the organization of the cytokeratin network but not the actin cytoskeleton within the vegetal cortex of *Xenopus* oocytes. We cannot exclude possibility that actin cytoskeleton is also

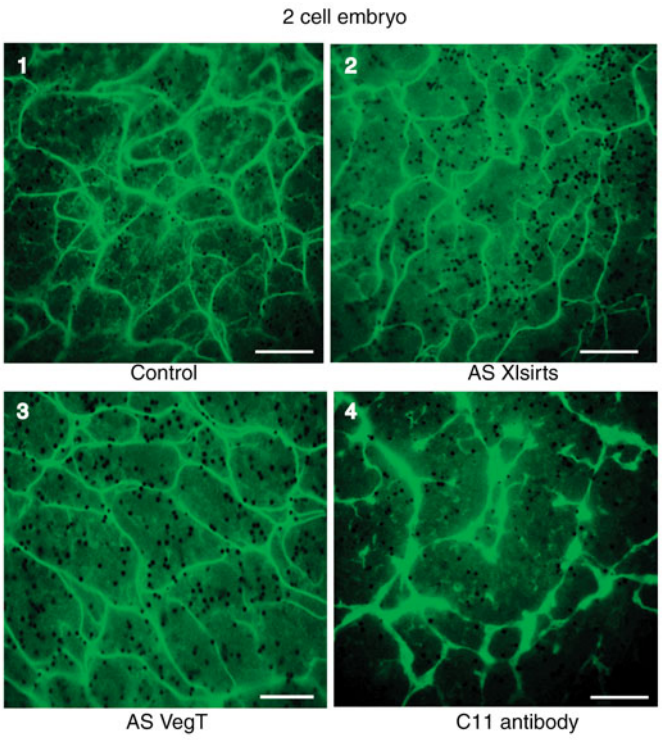

Fig. 9. Oocyte cytokeratin network disintegrated by the injection of antisense oligonucleotides or anti-pancytokeratin C11 antibody, reconstitutes spontaneously in cleaving embryos. Cleaving 2-cell stage embryos originating from control mock-injected oocytes (1), or oocytes injected with antisense Xlsirts ODNs (2), antisense VegT ODN (3), or anti-pancytokeratin C11 antibody (4) were produced by host transfer. Fixed embryos were stained with anti-pancytokeratin C11-FITC antibody and cortices of vegetal blastomeres were observed under fluorescent microscope. Intricate cytokeratin network comparable with control (1) reconstitutes in antisense Xlsirts (2) and antisense VegT embryos (3). In anti-pancytokeratin antibody embryos (4), the cytokeratin network also reconstitutes but looks different from control. Scale bars: 10 μm.

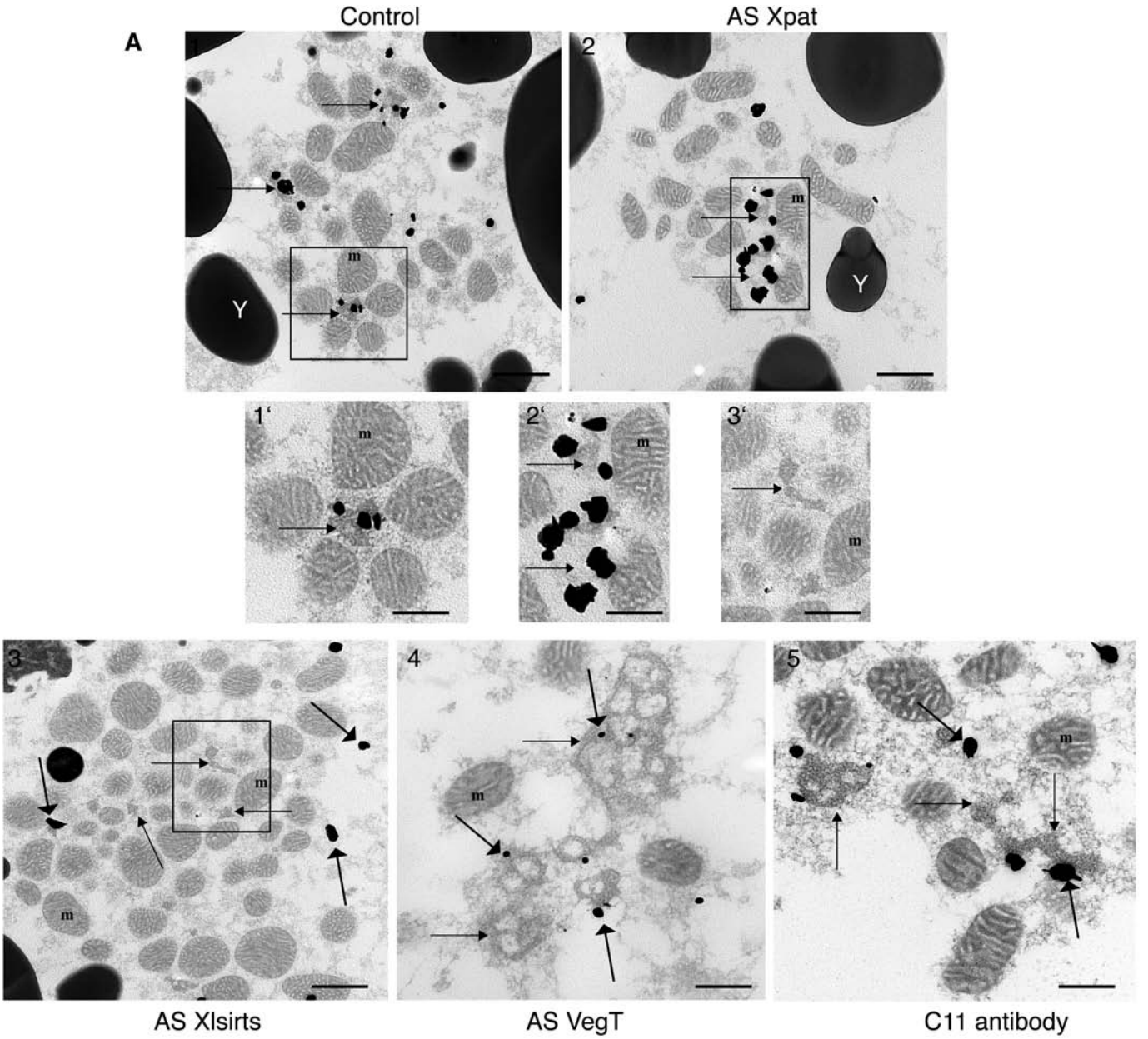

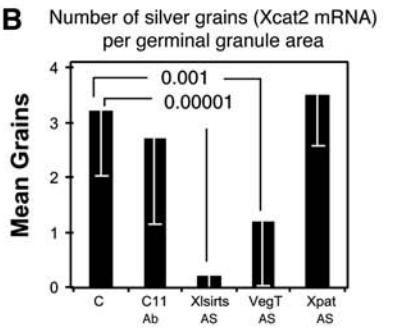

Fig. 10. Effect of antisense oligonucleotide and anti-pancytokeratin C11 antibody injection on the ultrastructure and molecular composition of germinal granules in four-cell embryos. (A) Electron microscopy of sections of germ plasm islands from four-cell embryos hybridized in situ, as whole mounts, with digoxigenin-labeled Xcat2 RNA probe. Hybridization signal was detected using nanogold-conjugated anti-digoxigenin antibody and silver enhancement (see Kloc et al., 2002a). In control uninjected embryos (1, inset 1′) and embryos injected with antisense Xpat ODN (2, inset 2′), the germinal granules (arrows) labeled with black silver grains (representing Xcat2 mRNA) are visible between mitochondria (m) and yolk platelets (Y). In embryos injected with antisense XIsirts ODNs (3, inset 3′) the germinal granules (small arrows) are devoid of label, and Xcat2 mRNA (black silver grains, large arrows) is located outside the germinal granules. In embryos injected with antisense VegT ODN (4), the germinal granules (small arrows) form huge aggregates containing low level of Xcat2 mRNA (small black silver grains, large arrows). In embryos injected with anti-pancytokeratin C11 antibody (5) the germinal granules form huge aggregates (small arrows), similar to aggregates in antisense VegT embryos, but heavily labeled with black silver grains (large arrows). Scale bars: 320 nm in 1-5, and 160 nm in 1′-3′. (B) Student's *t*-test statistical analysis of the number of silver grains (Xcat2 mRNA) associated with germinal granules. Each bar represents the average (with the standard deviation) number of silver grains counted in 10 independent samples in 0.25 μm^2 area of germinal granule in each experimental group. Number above the graph represents statistically significant ($P<0.05$) *P* value. The graph shows that the decrease in the number of silver grains (Xcat2 mRNA) present in the germinal granules of antisense XIsirts and antisense VegT embryos is statistically highly significant ($P=0.00001$ and $P=0.001$, respectively).

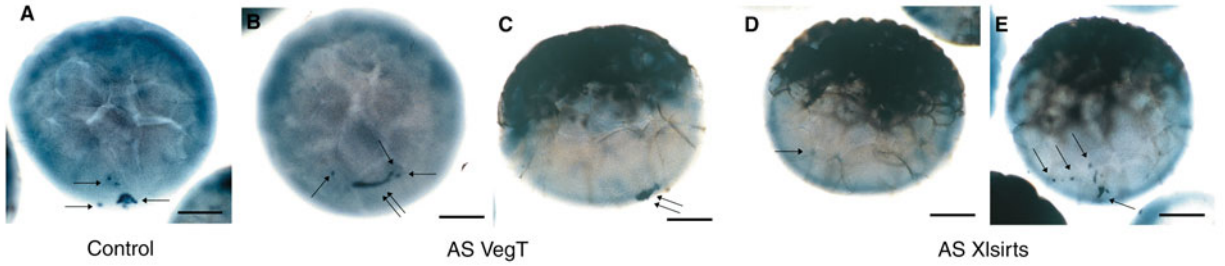

Fig. 11. Effect of antisense oligonucleotide injection on primordial germ cells (PGCs) in blastula. Whole-mount in situ hybridization with digoxigenin-labeled Xpat RNA probe. Embryos were acquired by host transfer and cleared to visualize their interior. In all embryos, the side view of blastulae is shown with the animal pole at the top and the vegetal pole at the bottom. In control embryo (A), the Xpat labeled islands of germ plasm (arrows) are visible in the compact group at the vegetal tip of the blastula. In antisense VegT-injected embryos (B,C), the germ plasm is visible as the large aggregates (double arrow, B and C) and also as small aggregates dispersed within the vegetal blastomeres (arrows, B). In antisense Xlsirts injected embryos (D,E), the germ plasm was either barely visible (arrow, D) or was dispersed over the larger surface of vegetal region of the blastula (arrows, E). Scale bars: 300 μm. The experiment was repeated three times with 20 embryos in each group.

affected but in more subtle way that was undetectable by our methods. We also found that destruction of Xlsirts or VegT RNA affects the cytokeratin network in different ways. Loss of Xlsirts RNA does not completely destroy the cytokeratin network in stage VI oocytes; rather, it causes a thinning of cytokeratin network and its collapse towards the yolk mass, with partial reformation of the network in activated eggs. By contrast, loss of VegT mRNA disrupts the network in stage VI oocytes, after which the network never reforms in activated eggs, but, interestingly, does reform in cleaving embryos, which suggests that, at least partially different mechanism(s) govern the cytokeratin network assembly in oocytes and embryos.

An important issue is whether Xlsirts and VegT RNAs interact directly with cytokeratin fibers. Our data show an intimate association of the localized Xlsirts and VegT RNA complexes with the cytokeratin network within the vegetal cortex. Our findings agree with previous findings by others that several different localized RNAs, including VegT, co-immunoprecipitate with the cytokeratin network (Alarcon and Elinson, 2001). Furthermore, we found that depletion of the Xlsirts RNA and especially VegT mRNA resulted in loss of integrity of the cytokeration network, and that exogenous VegT RNA was able to reconstitute cytokeratin network. We interpret this finding as an indication that these RNAs are integrated within the network holding the filaments together and/or are needed for the assembly of the network subunits (Fig. 12). Further analyses will be required to determine if the RNAs interact directly with the cytokeratin or if other proteins within the RNA complexes are required. The large size (0.5-1 μm) of these complexes suggests that they probably contain a multitude of RNA-associated proteins.

We propose that an intact cytokeratin network in stage VI oocytes and/or abundant cytokeratin foci in matured eggs prevent the untimely aggregation of germinal granules that normally takes place in embryos during early cleavage. This is supported by our data showing that the appearance of germinal granules in antisense VegT embryos is very similar to that in anti-cytokeratin antibody injected embryos. At present, there is no information on how cytokeratin filaments interact with the germ plasm or germinal granules. One possibility is that cytokeratin anchors the germinal granules, either directly or indirectly via other proteins. Thus, the severance of the cytokeratin network in oocytes injected with antisense VegT oligonucleotides or anti-cytokeratin antibody causes the release and untimely aggregation of germinal granules (Fig. 12). Another possibility is that cytokeratin itself does not have any structural or functional connection to the germinal granules but, as a structural component of the vegetal cortex, is necessary to preserve its integrity. If the latter possibility is true, then the untimely and premature aggregation of germinal granules is the result of intrinsic changes in the organization of the oocyte cortex in oocytes injected with antisense VegT oligonucleotides. Further studies are needed to explain how and why the depletion of Xlsirts RNA in stage VI oocytes caused the release of Xcat2 mRNA from the germinal granules in cleaving embryos and caused the changes in the morphology and the distribution of germ plasm islands in PGCs in blastula-stage embryos.

The importance of an intact cytokeratin network within the cortex has now been demonstrated in two studies. The first was a previous study showing that disruption of the cytokeratin in the oocyte cortex using anti-cytokeratin antibodies results in the release of several different RNAs (Alarcon and Elinson, 2001). The second is our current study, which demonstrated that the injection of anti-cytokeratin antibody and the depletion of Xlsirts and VegT RNAs (which specifically disrupted the cytokeratin cytoskeleton) had a dramatic effect on the morphogenesis and molecular composition of the germinal granules. This resulted in a phenotype affecting PGC formation in blastula embryos. The evidence that the VegT mRNA and not protein is serving a structural role is that antisense morpholino against VegT that inhibit translation of VegT protein (Heasman et al., 2001) did not produce this effect. Xlsirts does not encode protein, thus it must be functioning as an RNA.

Although the findings of this study apply to only a very specialized situation such as the anchoring of localized RNAs within the vegetal cortex of oocytes, it is quite likely that other RNAs play similar roles in both germ cells and somatic cells of other organisms. In the case of *Xenopus* oocytes, it is clear that integration of the RNAs into the cytoskeleton is of extreme importance for the proper formation and migration of the germ cells. In other systems, the role of the RNA-

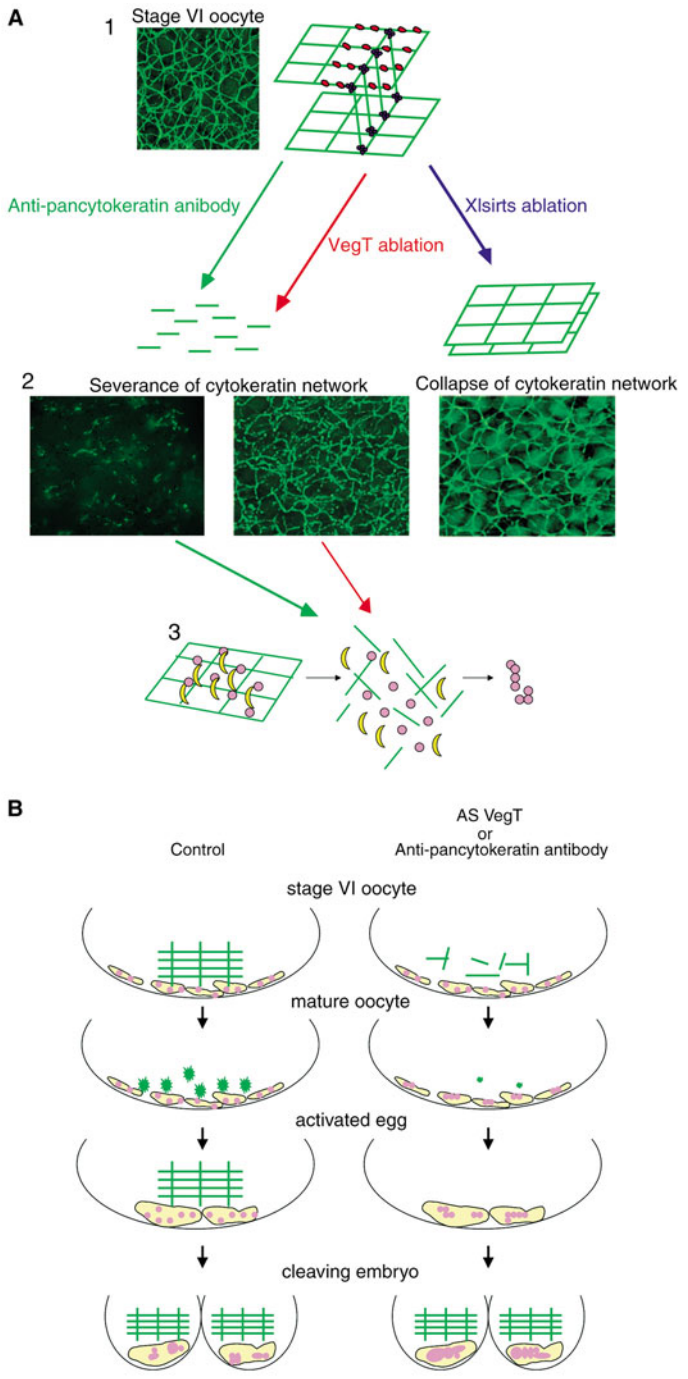

Fig. 12. Models of the effect of depletion of Xlsirts and VegT RNAs on the cytokeratin network and germinal granules. (A) The effect of Xlsirts RNA and VegT mRNA depletion, and of anti-cytokeratin antibody on the cytokeratin network and the germinal granules. In the cortex of stage VI oocytes, the cytokeratin (green) forms a complex, multi-layer network. The particles of VegT mRNA (red) and Xlsirts RNA (blue) are integrated into the network in RNA-specific pattern (1). The ablation of VegT mRNA or injection of anti-pancytokeratin antibody causes a severance of the network (2), which in turn, results in a premature aggregation of the germinal granules (3). The ablation of Xlsirts RNA results in the collapse of the network into a flattened, less complex sheet (2). The means of association of cytokeratin with germinal granules are unknown, but one possibility is that cytokeratin anchors germinal granules (pink spheres) indirectly, via an unknown binding protein(s) (yellow, 3). (B) The effect of VegT mRNA depletion and anti-cytokeratin antibody on the cytokeratin network and the germinal granule aggregation in oocytes and embryos. Control (left panel), and antisense VegT ODN or anti-cytokeratin C11 antibody injected (right panel) oocytes and embryos. Part of the vegetal cortex is shown. For simplicity, the cytokeratin is shown only in part of the cortex. In stage VI control oocytes, the germinal granules (pink spheres) are located in germ plasm islands (yellow) within the cortical network of cytokeratin filaments (green). In antisense VegT and anti-pancytokeratin antibody injected stage VI oocytes, the cytokeratin network is severed. In control mature oocytes, the cytokeratin network is replaced by cytokeratin foci with normal germinal granules and germ plasm. However, in mature antisense VegT- and anti-pancytokeratin antibody-injected oocytes, the germinal granules coalesce into long stringy aggregates. Upon egg activation, the cytokeratin network reconstitutes in control but not in antisense VegT-injected eggs, and only partially in anti-pancytokeratin antibody-injected eggs. In addition, the germ plasm islands aggregate into larger islands. In activated eggs, the germinal granules remain as small, separate entities in control eggs, and as stringy aggregates in antisense VegT and anti-pancytokeratin antibody-injected eggs. During early cleavage, the cytokeratin network is present both in control and in antisense VegT or anti-pancytokeratin antibody-injected embryos, and the germ plasm islands segregate to the vegetal apex of vegetal blastomeres. In control embryos, the germinal granules aggregate into larger, more complex germinal granules, and in antisense VegT or anti-pancytokeratin antibody-injected embryos, the stringy aggregates of germinal granules that were present in matured and activated eggs aggregate even further, resulting in the formation of extremely large aggregates.

cytoskeletal network may serve a different function; however, our results open up the exciting possibility of a new role for RNAs in maintaining the structural integrity of the cellular cytoskeleton.

This work was supported by grants from NSF (to L.D.E.), the Polish State Committee for Scientific Research-KBN grant BW/4/IZ/2002 (to K.W.), and Core Grant CA16672 and grant GM070357-01 to Sanjay Tyagi. We also thank Dr Sanjay Tyagi and Dr Salvatore Marras from the Department of Molecular Genetics (Public Health Research Institute, Newark, NJ) for their help in designing the molecular beacons and their helpful discussion of methods. We also thank Mr Kenneth Dunner, Jr, for his superb electron microscopy work.

References

Alarcon, V. B. and Elinson, R. P. (2001). RNA anchoring in the vegetal cortex of the *Xenopus* oocyte. *J. Cell Sci.* **114**, 1731-1741.

Bashirullah, A., Cooperstock, R. L. and Lipshitz, H. D. (1998). RNA localization in development. *Annu. Rev. Biochem.* **67**, 335-394.

Boccaccio, G. L., Carminatti, H. and Colman, D. R. (1999). Subcellular fractionation and association with the cytoskeleton of messengers encoding myelin proteins. *J. Neurosci. Res.* **58**, 480-491.

Bratu, D. P., Cha, B. J., Mhlanga, M. M., Kramer, F. R. and Tyagi, S. (2003).Visualizing the distribution and transport of mRNAs in living cells. *Proc. Natl. Acad. Sci. USA* **100**, 13308-13313.

Clarke, E. J. and Allan, V. J. (2003). Cytokeratin intermediate filament organisation and dynamics in the vegetal cortex of living *Xenopus* laevis oocytes and eggs. *Cell Mot. Cytoskel.* **56**, 13-26.

Elinson, R. P., King, M. L. and Forristall, C. (1993). Isolated vegetal cortex from *Xenopus* oocytes selectively retains localized RNAs. *Dev. Biol.* **160**, 554-562.

Forristall, C., Pondel, M., Chen, L. and King, M. L. (1995). Patterns of localization and cytoskeletal association of two vegetally localized RNAs, Vg1 and Xcat-2. *Development* **121**, 201-208.

Heasman, J., Holwill, S. and Wylie, C. C. (1991). In *Xenopus laevis: Practical Uses in Cell and Molecular Biology*. Vol. 36 (ed. B. K. Kay and H. B. Peng), pp. 213-230. New York: Academic Press.

Heasman, J., Wessely, O., Langland, R., Craig, E. J. and Kessler, D. S. (2001). Vegetal localization of maternal mRNAs is disrupted by VegT depletion. *Dev. Biol*. **240**, 377-386.

Horb, M. E. and Thomsen, G. H. (1997). A vegetally localized T-box transcription factor in *Xenopus* eggs specifies mesoderm and is essential for embryonic mesoderm formation. *Development* **124**, 1689-1698.

Hudson, C. and Woodland, H. R. (1998). Xpat, a gene expressed specifically in germ plasm and primordial germ cells of *Xenopus* laevis. *Mech. Dev*. **73**, 159-168.

Jankovics, F., Sinka, R., Lukacsovich, T. and Erdelyi, M. (2002). MOESIN crosslinks actin and cell membrane in Drosophila oocytes and is required for OSKAR anchoring. *Curr. Biol*. **12**, 2060-2065.

Jansen, R. P. (2001). mRNA localization: message on the move. *Nat. Rev. Mol. Cell. Biol*. **2**, 247-256.

Joseph, E. M. and Melton, D. A. (1998). Mutant Vg1 ligands disrupt endoderm and mesoderm formation in Xenopus embryos. *Development* **125**, 2677-2685.

Kessler, D. S. and Melton, D. A. (1995). Induction of dorsal mesoderm by soluble, mature Vg1 protein. *Development* **121**, 2155-2164.

King, M. L., Zhou, Y. and Bubunenko, M. (1999). Polarizing genetic information in the egg: RNA localization in the frog oocyte. *BioEssays* **21**, 546-557.

Kloc, M. and Etkin, L. D. (1994). Delocalization of Vg1 mRNA from the vegetal cortex in Xenopus oocytes after destruction of Xlsirts RNA. *Science* **265**, 1101-1103.

Kloc, M. and Etkin, L. D. (1995). Two distinct pathways for the localization of RNAs at the vegetal cortex in Xenopus oocytes. *Development* **121**, 287-297.

Kloc, M., Larabell, C. and Etkin, L. D. (1996). Elaboration of the messenger transport organizer pathway for localization of RNA to the vegetal cortex of Xenopus oocytes. *Dev. Biol*. **180**, 119-130.

Kloc, M., Larabell, C., Chan, A. P. and Etkin. L. D. (1998). Contribution of METRO pathway localized molecules to the organization of the germ cell lineage. *Mech. Dev*. **75**, 81-93.

Kloc, M., Bilinski, S., Chan, A. P., Allen, L. H., Zearfoss, N. R. and Etkin, L. D. (2001). RNA localization and germ cell determination in Xenopus. *Int. Rev. Cytol*. **203**, 63-91.

Kloc, M., Dougherty, M. T., Bilinski, S., Chan, A. P., Brey, E., King, M. L., Patrick, C. W. and Etkin, L. D. (2002a). Three-dimensional ultrastructural analysis of RNA distribution within germinal granules of *Xenopus*. *Dev. Biol*. **241**, 79-93.

Kloc, M., Zearfoss, N. R. and Etkin, L. D. (2002b). Mechanisms of subcellular mRNA localization. *Cell* **108**, 533-544.

Kloc, M., Bilinski, S., Dougherty, M. T., Brey, E. M. and Etkin, L. D. (2004). Formation, architecture and polarity of female germline cyst in Xenopus. *Dev. Biol*. **266**, 43-61.

Klymkowsky, M. W. and Maynell, L. A. (1989). MPF-induced breakdown of cytokeratin filament organization in the maturing *Xenopus* oocyte depends upon the translation of maternal mRNAs. *Dev. Biol*. **134**, 479-485.

Klymkowsky, M. W., Maynell, L. A. and Nislow, C. (1991). Cytokeratin phosphorylation, cytokeratin filament severing and the solubilization of the maternal mRNA Vg1. *J. Cell Biol*. **114**, 787-797.

Marikawa, Y., Li, Y. and Elinson, R. P. (1997). Dorsal determinants in the Xenopus egg are firmly associated with the vegetal cortex and behave like activators of the Wnt pathway. *Dev. Biol*. **191**, 69-79.

Marras, S. A., Gold, B., Kramer, F. R., Smith, I. and Tyagi, S. (2004). Real-time measurement of in vitro transcription. *Nucleic Acids Res*. **32**, e72.

Palacios, I. M. and St. Johnston, D. (2001). Getting the message across: the intracellular localization of mRNA in higher eukaryotes. *Annu. Rev. Cell. Dev. Biol.* **17**, 569-614.

Pondel, M. D. and King, M. L. (1988). Localized maternal mRNA related to transforming growth factor beta mRNA is concentrated in a cytokeratin-enriched fraction from Xenopus oocytes. *Proc. Natl. Acad. Sci. USA* **85**, 7612-7616.

Rebagliati, M. R., Weeks, D. L., Harvey, R. P. and Melton, D. A. (1985). Identification and cloning of localized maternal RNAs from Xenopus egg. *Cell* **42**, 769-777.

Shan, J., Munro, T. P., Barbarese, E., Carson, J. H. and Smith, R. (2003). A molecular mechanism for mRNA trafficking in neuronal dendrites. *J. Neurosci*. **23**, 8859-8866.

Stebbings, H. (2001). Cytoskeleton-dependent transport and localization of mRNA. *Int. Rev. Cytol.* **211**, 1-31.

Tyagi, S. and Kramer, F. R. (1996). Molecular beacons: probes that fluoresce upon hybridization. *Nat. Biotechnol*. **14**, 303-308.

Wessely, O. and de Roberis, E. M. (2000). The *Xenopus* homologue of Bicaudal-C is a localized maternal mRNA that can induce endoderm formation. *Development* **127**, 2053-2062.

Xanthos, J. B., Kofron, M., Wylie, C. and Heasman, J. (2001). Maternal VegT is the initiator of a molecular network specifying endoderm in *Xenopus* laevis. *Development* **128**, 167-180.

Yisraeli, J. K. and Melton, D. A. (1988). The maternal mRNA Vg1 is correctly localized following injection into *Xenopus* oocytes. *Nature* **336**, 592-595.

Yisraeli, J. K., Sokol, S. and Melton, D. A. (1990). A two-step model for the localization of maternal mRNA in *Xenopus* oocytes: involvement of microtubules and microfilaments in the translocation and anchoring of Vg1 mRNA. *Development* **108**, 289-298.

Zearfoss, N. R., Chan, A. P., Wu, C. F., Kloc, M. and Etkin, L. D. (2004). Hermes is a localized factor regulating cleavage of vegetal blastomeres in *Xenopus* laevis. *Dev. Biol*. **267**, 60-71.

Zhang, J. and King, M. L. (1996). Xenopus VegT RNA is localized to the vegetal cortex during oogenesis and encodes a novel T-box transcription factor involved in mesodermal patterning. *Development* **122**, 4119-4129.

Zhao, W. M., Jiang, C., Kroll, T. T. and Huber, P. W. (2001). A proline-rich protein binds to the localization element of Xenopus Vg1 mRNA and to ligands involved in actin polymerization. *EMBO J*. **20**, 2315-2325.